Distributionally Robust Resilient Operation of Integrated Energy Systems Using Moment and Wasserstein Metric for Contingencies

Yizhou Zhou, *Member, IEEE*, Zhinong Wei, *Member, IEEE*, Mohammad Shahidehpour, *Life Fellow, IEEE*, and Sheng Chen, *Member, IEEE*

***Abstract*—Extreme weather events pose a serious threat to energy distribution systems. We propose a distributionally robust optimization model for the resilient operation of the integrated electricity and heat energy distribution systems in extreme weather events. We develop a strengthened ambiguity set that incorporates both moment and Wasserstein metric information of uncertain contingencies, which provides a more accurate characterization of the true probability distribution. We first recast the proposed model into an equivalent framework which is similar to a conventional two-stage robust model and then utilize a modified column-and-constraint generation algorithm to solve the recast model. Numerical results from three test systems validate the enhanced resilience of the distributionally robust approach, the reduced conservatism of the strengthened ambiguity set, and the computational efficiency of the proposed solution algorithm.**

***Index Terms*—Distributionally robust optimization, resilience, integrated energy system, ambiguity set, column-and-constraint generation algorithm.**

NOMENCLATURE

Acronyms

CHP	Combined heat and power.
PDN	Power distribution network.
DHN	District heating network.
DR	Distributionally robust.

Indices

t, τ	Subscript indices of time periods.
g	Subscript index of CHP units.
b	Subscript index of heat boilers.
m	Subscript index of corner points.
i, j, h	Subscript indices of buses in PDN.
n	Subscript index of nodes in DHN.
p	Subscript index of pipelines in DHN.

Variables

z	Binary variable indicating whether branch is on outage (0) or not (1).
$x/u/v$	Binary variable indicating whether CHP unit is on/start-up/shut-down (1) or not (0).
$P^{\mathrm{CHP}}/H^{\mathrm{CHP}}$	Electric/thermal power output of CHP unit.
H^{HB}	Thermal power output of heat boiler.
k^{LS}	Load shedding ratio.
k^{CP}	Combination coefficient of corner point.
P_{ij}/Q_{ij}	Active/reactive power flow of branch *i–j*.
V	Voltage magnitude.
$T^{\mathrm{S}}/T^{\mathrm{R}}$	Supply/return temperature.
$T^{\mathrm{in}}/T^{\mathrm{out}}$	Inlet/outlet temperature of pipeline.
T^{mix}	Mixture temperature at confluence node.

Parameters

$C^{\mathrm{SU}}/C^{\mathrm{SD}}/C^{\mathrm{NL}}$	Start-up/shut-down/no-load cost of CHP unit.
C^{HB}	Fuel cost of heat boiler.
C^{LS}	Load shedding cost.
c^{CP}	Corresponding fuel cost of corner point.
UT/DT	Minimum up-/down-time of CHP unit.
RU/RD	Ramp-up/-down limit of CHP unit.
SU/SD	Start-up/shut-down ramp limit of CHP unit.
$P^{\mathrm{CP}}/H^{\mathrm{CP}}$	Electric/thermal power output of corner point.
$P^{\mathrm{L}}/Q^{\mathrm{L}}$	Active/reactive load.
r_{ij}/x_{ij}	Resistance/reactance of branch *i–j*.
V^0	Voltage magnitude at slack bus.
H^{L}	Heat load.
c^{P}	Specific heat capacity of water.
$m^{\mathrm{S}}/m^{\mathrm{L}}$	Mass flow rate of heat source/load.
m	Mass flow rate within pipeline.
T^{A}	Ambient temperature.
λ	Heat transfer coefficient of pipeline.
L	Length of pipeline.

Manuscript received July 9, 2020; revised November 9, 2020 and December 25, 2020; accepted January 2, 2021. Date of publication January 6, 2021; date of current version June 18, 2021. Paper no. TPWRS-01144-2020. This work was supported by NSFC under Grant 51877071. *(Corresponding author: Zhinong Wei.)*

Yizhou Zhou, Zhinong Wei, and Sheng Chen are with the College of Energy and Electrical Engineering, Hohai University, Nanjing 210098, China (e-mail: hhuzhouyizhou@foxmail.com; wzn_nj@263.net; chenshenghhu@163.com).

Mohammad Shahidehpour is with the Electrical and Computer Engineering Department, Illinois Institute of Technology, Chicago, IL 60616 USA (e-mail: ms@iit.edu).

Color versions of one or more figures in this article are available at https://doi.org/10.1109/TPWRS.2021.3049717.

Digital Object Identifier 10.1109/TPWRS.2021.3049717

Sets

S_i^{CHP} Set of CHP units at bus i.
S_n^{CHP} Set of CHP units at node n.
S_n^{HB} Set of heat boilers at node n.
$S_i^{\mathrm{B,d}}$ Set of downstream buses connecting to bus i.
$S_n^{\mathrm{P,s}}$ Set of pipelines starting at node n.
$S_n^{\mathrm{P,e}}$ Set of pipelines ending at node n.

I. Introduction

POWER outages caused by severe weather events have resulted in enormous economic losses. For instance, the annual cost of weather-related power outages in the U.S. was \$18-\$33 billion between 2003 and 2012, and 90% of power outages occurred in distribution systems [1]. This issue is becoming increasingly serious owing to the effects of climate changes on the gradually growing frequency, intensity, and duration of severe weather events worldwide. For example, the U.S. suffered 119 severe weather-related disasters where overall economic losses exceeded \$1 billion in the 2010s, which were more frequent than those in the 2000s and 1980s by factors of roughly two and four, respectively [2]. Moreover, this issue is further related to the recent developments associated with the proliferation of combined heat and power (CHP) units and district heating networks (DHNs) in urban areas. The additional interest in DHNs has created integrated energy distribution systems that allow the coordinated operations of power distribution networks (PDNs) and DHNs. The integration promotes higher energy efficiency, lower operation costs, and lower carbon emissions than those of individual networks operating independently [3]. Accordingly, it is of vital urgency and importance to improve the resilience of the integrated electricity and heat energy distribution systems in extreme weather events.

Existing studies have extended the conventional resilience enhancement measures developed for electric power systems [4], [5] to integrated energy systems. Amirioun *et al.* [6] presented a resilience-oriented proactive measure against hurricanes for electricity and natural gas distribution systems. Shao *et al.* [7] developed a robust optimization approach for the integrated planning of electricity and natural gas systems to enhance the system resilience against extreme events. Yan *et al.* [8] accommodated random outages of integrated electricity and natural gas systems by developing a robust coordinated operation strategy. Li *et al.* [9] formulated a robust cooperation optimization model to hedge integrated power distribution and natural gas systems against the worst $N-k$ contingencies.

In addition to the conventional stochastic programming [10] and robust optimization [11], [12], distributionally robust (DR) optimization [13], [14] has been developed in recent years as a novel approach to address uncertainties. DR optimization incorporates the available probability distribution information into an ambiguity set to characterize the true probability distribution of uncertain parameters. Accordingly, it eliminates the inherent dependence of stochastic programming on exact probability distributions and reduces the solution conservatism of robust optimization. Presently, DR approaches adopt two main types of ambiguity sets, that is, moment- and metric-based ambiguity sets. Moment-based ambiguity sets accommodate moment information of probability distributions [15], [16], while metric-based ambiguity sets specify the closeness of probability distributions to an empirical distribution through a given statistical distance metric [17]. The Wasserstein metric is a typical distance metric.

A few studies have applied DR approaches to address the uncertainties of renewable power outputs and loads in integrated energy systems. Zhou *et al.* [18] proposed a DR approach to determine the optimal day-ahead unit commitment in coordinated electricity and district heating networks, where a moment-based ambiguity set was constructed for variable renewable power outputs. He *et al.* [19] presented a moment-based DR scheduling model for integrated electricity and natural gas systems with load uncertainties. Wang *et al.* [20] captured uncertain wind power generations using a Wasserstein metric-based ambiguity set in a DR optimal power-gas flow model. Other works have studied DR models for hedging against uncertain contingencies in electric power systems. Zhao *et al.* [21] proposed a DR contingency-constrained unit commitment model with a moment-based ambiguity set. Babaei *et al.* [22] presented a moment-based DR model for distribution network configuration problems with random contingencies.

Despite strenuous efforts, several gaps remain in existing works. First, while numerous studies have applied conventional robust approaches to address random contingencies in integrated energy systems, few studies have explored the merits of applying DR approaches for this purpose. Resilience researches of integrated electricity and heat energy systems are also rather limited. Second, existing DR approaches have exclusively employed either moment-based or metric-based ambiguity sets, even though both have their own disadvantages. Moment-based ambiguity sets that consider only moment information do not provide a detailed characterization of the true probability distribution, while metric-based ambiguity sets tend to perform well when massive historical data are available, but often provide meager performances for relatively sparse historical data, such as extreme weather events with a low probability. Finally, linear decision rules have been applied to solve either moment-based or Wasserstein metric-based DR models of integrated energy systems, despite that linear decision rules are only conservative approximations of fully adaptive approaches.

In this paper, we address the above gaps by making the following three key contributions.

1) We propose a DR model for the resilient operation of the integrated electricity and heat energy distribution systems in impending extreme weather events.
2) We construct a strengthened ambiguity set that incorporates both moment and Wasserstein metric information of uncertain contingencies. This set provides a more accurate characterization of the true probability distribution, and thus generates a more trustworthy and less conservative solution.
3) We first transform the proposed DR model into an equivalent framework, which is similar to a conventional two-stage robust model, and then utilize a modified column-and-constraint generation algorithm to solve the recast model. The utilized algorithm is a fully adaptive approach that will not lead to conservative solutions.

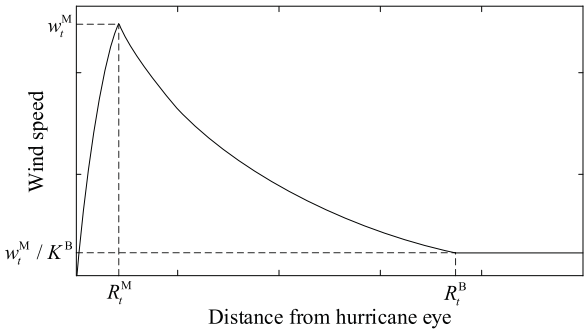

Fig. 1. Hurricane speed with respect to distance from hurricane eye.

The remainder of this paper is organized as follows. Section II details the mathematical formulation. Section III presents the solution methodology. Section IV provides three case studies. Section V concludes.

II. Proposed Model Formulation

We begin this section with the hurricane and the branch outage probability model, which are crucial for the generation of ambiguity set parameters. Then, we present the strengthened ambiguity set. Finally, we formulate the DR model.

Before providing the model formulation, we outline the key considerations and assumptions as follows.

1) We concentrate on hurricanes because they are the primary extreme weather events that can cause extensive damages to power system infrastructures [1].
2) We assume that heat systems are invulnerable to hurricanes because heat pipelines are normally deployed underground.
3) We assume the entire integrated energy distribution system is exposed to the same weather condition considering the relatively small footprint of distribution systems.
4) We assume the branches will be on outage in the remaining periods of the hurricane day if damaged on that day, because the repair of damaged branches normally takes longer than a day during a hurricane [23]. As such, the restoration progress can be omitted in the day-ahead scheduling problem for the upcoming hurricane day.

A. Hurricane Model

The wind speed w_t at the vicinity of the integrated energy distribution system is calculated using a function of the distance from the hurricane eye to the distribution system [24]. This function is depicted in Fig. 1 and presented as follows.

$$w_t = \begin{cases} K^{\mathrm{C}} w_t^{\mathrm{M}} & \\ \left\{1 - \exp\left[-\frac{1}{R_t^{\mathrm{M}}} \ln\left(\frac{K^{\mathrm{C}}}{K^{\mathrm{C}}-1}\right) D_t\right]\right\} & \forall 0 \le D_t < R_t^{\mathrm{M}} \\ w_t^{\mathrm{M}} \exp\left[-\frac{\ln K^{\mathrm{B}}}{R_t^{\mathrm{B}} - R_t^{\mathrm{M}}}\left(D_t - R_t^{\mathrm{M}}\right)\right] & \forall R_t^{\mathrm{M}} \le D_t \le R_t^{\mathrm{B}} \\ 0 & \forall D_t > R_t^{\mathrm{B}} \end{cases} \tag{1a}$$

Here, K^{C} and K^{B} are model parameters that reflect the hurricane speed and the hurricane boundary, respectively, w_t^{M} denotes the maximum hurricane speed, R_t^{M} and R_t^{B} represent the distances from the hurricane eye to the point of the maximum wind speed and the hurricane boundary, respectively, and D_t represents the distance from the hurricane eye to the distribution system. Accordingly, w_t can be calculated based on the hurricane parameters w_t^{M}, R_t^{M}, and R_t^{B} when the hurricane eye location is identified. In this paper, model parameters K^{C} and K^{B} are fixed at 1.14 and 10, respectively, and time-varying hurricane parameters w_t^{M}, R_t^{M}, R_t^{B} and hurricane eye locations are generated using the approach and historical hurricane data provided in [24].

The wind speed upper bound $\bar{w}_t$ is calculated as

$$\bar{w}_t = \begin{cases} K^{\mathrm{C}} \bar{w}_t^{\mathrm{M}} & \\ \left\{1 - \exp\left[-\frac{1}{\bar{R}_t^{\mathrm{M}}} \ln\left(\frac{K^{\mathrm{C}}}{K^{\mathrm{C}}-1}\right) D_t\right]\right\} & \forall 0 \le D_t < \bar{R}_t^{\mathrm{M}} \\ \bar{w}_t^{\mathrm{M}} & \forall \bar{R}_t^{\mathrm{M}} \le D_t < \bar{R}_t^{\mathrm{M}} \\ \bar{w}_t^{\mathrm{M}} \exp\left[-\frac{\ln K^{\mathrm{B}}}{\bar{R}_t^{\mathrm{B}} - \bar{R}_t^{\mathrm{M}}}\left(D_t - \bar{R}_t^{\mathrm{M}}\right)\right] & \forall \bar{R}_t^{\mathrm{M}} \le D_t \le \bar{R}_t^{\mathrm{B}} \\ 0 & \forall D_t > \bar{R}_t^{\mathrm{B}} \end{cases} \tag{1b}$$

B. Branch Outage Probability Model

A distribution branch fails if any one of its components fails. Here, poles are considered as the primary branch component which is subject to failure. Assuming that damages sustained by poles are independent, the damage probability $p_{ij,t}^{\mathrm{D}}$ of branch *i–j* is calculated as

$$p_{ij,t}^{\mathrm{D}} = 1 - \prod_{q} \left(1 - p_{ij,q,t}^{\mathrm{P}}(w_t)\right), \tag{2a}$$

where $p_{ij,q,t}^{\mathrm{P}}(w_t)$ is the damage probability of pole q supporting branch *i–j*. $p_{ij,q,t}^{\mathrm{P}}(w_t)$ complies with the fragility curve, which is typically modeled as a lognormal cumulative distribution function of w_t [5]:

$$p_{ij,q,t}^{\mathrm{P}}(w_t) = \Phi\left[\frac{\ln\left(w_t/\mu\right)}{\sigma}\right], \tag{2b}$$

where μ and σ are the median and logarithmic standard deviation of the lognormal distribution.

Note that the damage condition $F_{ij,t}^{\mathrm{D}}$ of branch *i–j* follows a Bernoulli distribution with the probability $p_{ij,t}^{\mathrm{D}}$ for each period, and the branch is on outage if damaged in any prior periods. That is, $z_{ij,t} = 0$ if $F_{ij,\tau}^{\mathrm{D}} = 1$ for any $\tau \le t$. Besides, the outage probability $p_{ij,t}$ of branch *i–j* is calculated considering the time cumulative effect of $p_{ij,t}^{\mathrm{D}}$ as

$$p_{ij,t} = 1 - \prod_{\tau \le t} \left(1 - p_{ij,\tau}^{\mathrm{D}}\right). \tag{2c}$$

C. Strengthened Ambiguity Set

Here, we first provide the procedure for obtaining the branch outage probability upper bound $\bar{p}_{ij,t}$ and the branch outage

samples $z^{\mathrm{E}}_{s,ij,t}$, which are essential moment and Wasserstein metric data, respectively. The detailed procedure is given below.

Step 1: Generate hurricane parameter samples $w^{\mathrm{M}}_{s,t}$, $R^{\mathrm{M}}_{s,t}$, $R^{\mathrm{B}}_{s,t}$ and hurricane eye locations. Obtain wind speed samples $w_{s,t}$ from (1a) and corresponding upper bound $\bar{w}_t$ from (1b).

Step 2: Obtain the branch damage probability upper bound $\bar{p}^{\mathrm{D}}_{ij,t}$ from (2a) and (2b) by substituting $\bar{w}_t$ for w_t. Similarly, obtain branch damage probability samples $p^{\mathrm{D}}_{s,ij,t}$ using $w_{s,t}$.

Step 3: Obtain the branch outage probability upper bound $\bar{p}_{ij,t}$ from (2c) by substituting $\bar{p}^{\mathrm{D}}_{ij,t}$ for $p^{\mathrm{D}}_{ij,t}$. Generate branch damage condition samples $F^{\mathrm{D}}_{s,ij,t}$ from the Bernoulli distribution of $p^{\mathrm{D}}_{s,ij,t}$ to obtain branch outage samples $z^{\mathrm{E}}_{s,ij,t}$ by setting $z^{\mathrm{E}}_{s,ij,t}=0$ when $F^{\mathrm{D}}_{s,ij,\tau}=1$ for all $t\geq\tau$ and setting $z^{\mathrm{E}}_{s,ij,t}=1$ otherwise.

Through the above procedure, the hurricane data are characterized by branch outage data, and thereby can be considered in the DR resilient operation model.

Then, we construct the strengthened ambiguity set F that incorporates both moment and Wasserstein metric information as follows:

$$F=\left\{\mathrm{P}\in P(\Omega)\;\middle|\;\begin{array}{c}\mathrm{E}_{\mathrm{P}}(1-z_{ij,t})\leq\bar{p}_{ij,t}\\ d_W(\mathrm{P},\mathrm{P}^{\mathrm{E}})\leq\theta\end{array}\right\},\tag{3a}$$

where the support set Ω is defined as

$$\Omega=\left\{z_{ij,t}\in\mathrm{R}^I\;\middle|\;\begin{array}{c}\sum\limits_{ij}z_{ij,t}\geq N-k\\ z_{ij,t}\leq z_{ij,\tau}\quad\forall t>\tau\end{array}\right\}.\tag{3b}$$

Here, P and P^{E} denote the true and empirical branch outage probability distributions, respectively, $P(\Omega)$ represents the set of all probability distributions on a σ-algebra of Ω, θ is the Wasserstein radius representing the distance between P and P^{E}, which controls the conservatism of solutions and is discussed in detail later. P^{E} serves as an estimate of P and is defined as $\mathrm{P}^{\mathrm{E}}=\sum_s p_s\delta(z^{\mathrm{E}}_{s,ij,t})$, where p_s is the probability of samples $z^{\mathrm{E}}_{s,ij,t}$ and $\delta(z^{\mathrm{E}}_{s,ij,t})$ indicates the Dirac measure on $z^{\mathrm{E}}_{s,ij,t}$. Ω is designated in (3b) considering $N-k$ contingencies, i.e., no more than k branches are on outage simultaneously. The value of k can be selected according to branch outage samples. Specifically, we can set k to the maximum number of branch outages in all samples to ensure that Ω supports all plausible scenarios. The first line of (3a) restricts the first-order moment of $p_{ij,t}$ to an upper limit $\bar{p}_{ij,t}$. We adopt the upper bound of the first-order moment herein because historical hurricane data are not sufficiently available to provide accurate estimations of the second-order moment and actual moment values. The second line of (3a) restricts P to reside within a Wasserstein ball with a center P^{E} and radius θ. The Wasserstein metric $d_W(\mathrm{P},\mathrm{P}^{\mathrm{E}})$ is defined as

$$\begin{aligned}&d_W(\mathrm{P},\mathrm{P}^{\mathrm{E}})\\&=\inf_{\Pi}\left\{\int_{z_{ij,t}\in\Omega}\int_{z^{\mathrm{E}}_{ij,t}\in\Omega}\left\|z_{ij,t}-z^{\mathrm{E}}_{ij,t}\right\|\Pi\left(dz_{ij,t},dz^{\mathrm{E}}_{ij,t}\right)\right\},\end{aligned}\tag{3c}$$

where Π is the joint distribution of $z_{ij,t}$ and $z^{\mathrm{E}}_{ij,t}$ with marginal distributions P and P^{E}, respectively, and $\|\cdot\|$ is the norm operator. We adopt the l_1 norm in this paper because of its computational tractability [17].

Intuitively, P^{E} converges to P, such that θ approaches 0 as more data are available. Thus, θ normally depends on the sample size N^{S}. Here, θ is chosen to satisfy the following expression:

$$\mathrm{P}\left(d_W(\mathrm{P},\mathrm{P}^{\mathrm{E}})\leq\theta\right)\geq1-\exp\left(-N^{\mathrm{S}}\frac{\theta^2}{C^2}\right),\tag{3d}$$

such that P^{E} converges to P exponentially with increasing N^{S} [17]. As such, θ can be expressed with a given confidence level η as

$$\theta=C\sqrt{\frac{1}{N^{\mathrm{S}}}\ln\left(\frac{1}{1-\eta}\right)},\tag{3e}$$

where C is a constant that can be obtained directly by solving the following optimization problem of κ:

$$C=\min_{\kappa>0}2\sqrt{\frac{1}{2\kappa}\left\{1+\ln\left[\sum_s p_s\exp\left(\kappa\left\|z^{\mathrm{E}}_{s,ij,t}-z^{\mathrm{M}}_{ij,t}\right\|^2\right)\right]\right\}}.\tag{3f}$$

Here, $z^{\mathrm{M}}_{ij,t}$ is the sample mean.

D. Distributionally Robust Model

The DR model is to determine the optimal day-ahead resilience operation of integrated energy distribution systems for the upcoming hurricane day. The model corresponds to a two-stage optimization problem. The first-stage problem determines day-ahead unit commitment decisions of CHP units as preventive measures one day before the hurricane day. In the second stage, system re-dispatch actions are implemented as corrective measures immediately after observing branch outages during the hurricane. The first-stage problem is expressed as:

$$\begin{aligned}\min_{\mathbf{x}}\;&\sum_t\sum_g\left(C^{\mathrm{SU}}_g u_{g,t}+C^{\mathrm{SD}}_g v_{g,t}+C^{\mathrm{NL}}_g x_{g,t}\right)\\&+\sup_{\mathrm{P}\in F}\mathrm{E}_{\mathrm{P}}\left[Q(\mathbf{x},\mathbf{z})\right],\end{aligned}\tag{4a}$$

$$\text{s.t. } x_{g,t}-x_{g,t-1}=u_{g,t}-v_{g,t},\tag{4b}$$

$$x_{g,t}\geq u_{g,\tau}\quad\forall\tau\leq t\leq\tau+UT_g-1,\tag{4c}$$

$$1-x_{g,t}\geq v_{g,\tau}\quad\forall\tau\leq t\leq\tau+DT_g-1,\tag{4d}$$

where $\mathbf{x}=\{x_{g,t},\,u_{g,t},\,v_{g,t}\}$ denotes the first-stage binary variables determining CHP unit commitment decisions, and $\mathbf{z}$ contains random branch outages $z_{ij,t}$. The first-stage objective function (4a) is subject to binary variable logical relation constraint (4b) and the respective minimum up- and down-time constraints (4c) and (4d) of CHP units. Here, the first term in (4a) represents the sum of start-up, shut-down, and no-load costs of CHP units, and the second term represents the worst-case expectation of the second-stage operation cost $Q(\mathbf{x},\mathbf{z})$, stated

as

$$Q(\mathbf{x},\mathbf{z}) = \min_{\mathbf{y}} \sum_{t} \left(\begin{array}{l} \sum\limits_{g} f_g^{\mathrm{CHP}}(P_{g,t}^{\mathrm{CHP}}, H_{g,t}^{\mathrm{CHP}}) \\ + \sum\limits_{b} C_b^{\mathrm{HB}} H_{b,t}^{\mathrm{HB}} + \sum\limits_{i} C_i^{\mathrm{LS}} k_{i,t}^{\mathrm{LS}} P_{i,t}^{\mathrm{L}} \end{array} \right), \tag{4e}$$

where $\mathbf{y} = \{P_{g,t}^{\mathrm{CHP}}, H_{g,t}^{\mathrm{CHP}}, H_{b,t}^{\mathrm{HB}}, k_{i,t}^{\mathrm{L,S}}, k_{g,m,t}^{\mathrm{CP}}, P_{ij,t}, Q_{ij,t}, V_{i,t}, T_{n,t}^{\mathrm{S}}, T_{n,t}^{\mathrm{R}}, T_{p,t}^{\mathrm{in}}, T_{p,t}^{\mathrm{out}}, T_{n,t}^{\mathrm{mix}}\}$ denotes the second-stage operation variables, and $f_g^{\mathrm{CHP}}(P_{g,t}^{\mathrm{CHP}}, H_{g,t}^{\mathrm{CHP}})$ is the fuel cost function of CHP units. The second-stage objective function (4e) comprises the CHP fuel, heat boiler fuel, and load shedding costs, which is subject to the following operational models and constraints.

1) CHP Model: The electric and thermal power outputs of extraction steam turbine CHP units must be constrained to within a convex polyhedron operating region and can therefore be governed by a convex combination of corner points in the operating region as follows [25]:

$$P_{g,t}^{\mathrm{CHP}} = \sum_{m} k_{g,m,t}^{\mathrm{CP}} P_{g,m}^{\mathrm{CP}}, \tag{4f}$$

$$H_{g,t}^{\mathrm{CHP}} = \sum_{m} k_{g,m,t}^{\mathrm{CP}} H_{g,m}^{\mathrm{CP}}, \tag{4g}$$

where

$$0 \le k_{g,m,t}^{\mathrm{CP}} \le 1, \tag{4h}$$

$$\sum_{m} k_{g,m,t}^{\mathrm{CP}} = x_{g,t}. \tag{4i}$$

The fuel cost of CHP units can be approximated as a piecewise linear function by a convex combination of corner points [25]:

$$f_g^{\mathrm{CHP}}(P_{g,t}^{\mathrm{CHP}}, H_{g,t}^{\mathrm{CHP}}) = \sum_{m} k_{g,m,t}^{\mathrm{CP}} c_{g,m}^{\mathrm{CP}}. \tag{4j}$$

The ramping limits of CHP units are:

$$P_{g,t}^{\mathrm{CHP}} - P_{g,t-1}^{\mathrm{CHP}} \le RU_g x_{g,t-1} + SU_g u_{g,t}, \tag{4k}$$

$$P_{g,t-1}^{\mathrm{CHP}} - P_{g,t}^{\mathrm{CHP}} \le RD_g x_{g,t} + SD_g v_{g,t}. \tag{4l}$$

2) PDN Model: The electric power flows in the PDN with a radial topology are described by the linearized DistFlow branch model [26]. This model is more appropriate than the DC power flow model owing to the incorporation of reactive power and voltage magnitudes [27], and therefore has been broadly implemented in power distribution systems [4], [5] and integrated electricity and heat energy distribution systems [3], [28]. The linearized DistFlow branch model is given as

$$\sum_{g \in S_j^{\mathrm{CHP}}} P_{g,t}^{\mathrm{CHP}} + P_{ij,t} = \sum_{h \in S_j^{\mathrm{B,d}}} P_{jh,t} + \left(1 - k_{j,t}^{\mathrm{LS}}\right) P_{j,t}^{\mathrm{L}}, \tag{4m}$$

$$\sum_{g \in S_j^{\mathrm{CHP}}} Q_{g,t}^{\mathrm{CHP}} + Q_{ij,t} = \sum_{h \in S_j^{\mathrm{B,d}}} Q_{jh,t} + \left(1 - k_{j,t}^{\mathrm{LS}}\right) Q_{j,t}^{\mathrm{L}}, \tag{4n}$$

$$V_{i,t} - \left(P_{ij,t} r_{ij} + Q_{ij,t} x_{ij}\right)/V^0 - V_{j,t} + M\left(1 - z_{ij,t}\right) \ge 0, \tag{4o}$$

$$V_{i,t} - \left(P_{ij,t} r_{ij} + Q_{ij,t} x_{ij}\right)/V^0 - V_{j,t} - M\left(1 - z_{ij,t}\right) \le 0. \tag{4p}$$

(4m) and (4n) represent the PDN active and reactive power balance, respectively. (4o) and (4p) represent the relation of voltage magnitudes and branch power flows, where the bus voltages at the two ends of a damaged branch are decoupled using the big *M* approach. The active and reactive branch power flow limits considering network connectivity are expressed as

$$-\bar{P}_{ij} z_{ij,t} \le P_{ij,t} \le \bar{P}_{ij} z_{ij,t}, \tag{4q}$$

$$-\bar{Q}_{ij} z_{ij,t} \le Q_{ij,t} \le \bar{Q}_{ij} z_{ij,t}. \tag{4r}$$

The voltage magnitudes are limited within secure ranges:

$$\underline{V}_i \le V_{i,t} \le \bar{V}_i. \tag{4s}$$

Finally, the load shedding ratio limit is stated as

$$0 \le k_{i,t}^{\mathrm{LS}} \le 1. \tag{4t}$$

3) DHN Model: The DHN is assumed to be operated under a constant flow and variable temperature (CF-VT) control mode [29], [30]. Under this control mode, circulating water temperatures are adjustable, while mass flow rates are fixed. Note that the DHN model can be extended to consider the thermal inertia [31], the variable flow control strategy [32], and the demand response strategy [33], [34] without the loss of the applicability of the proposed approach. The DHN model with symmetric supply and return pipelines is given as

$$\sum_{g \in S_n^{\mathrm{CHP}}} H_{g,t}^{\mathrm{CHP}} + \sum_{b \in S_n^{\mathrm{HB}}} H_{b,t}^{\mathrm{HB}} = c^{\mathrm{P}} m_{n,t}^{\mathrm{S}} \left(T_{n,t}^{\mathrm{S}} - T_{n,t}^{\mathrm{R}}\right), \tag{4u}$$

$$H_{n,t}^{\mathrm{L}} = c^{\mathrm{P}} m_{n,t}^{\mathrm{L}} \left(T_{n,t}^{\mathrm{S}} - T_{n,t}^{\mathrm{R}}\right), \tag{4v}$$

$$T_{p,t}^{\mathrm{out}} = \left(T_{p,t}^{\mathrm{in}} - T_t^{\mathrm{A}}\right) \exp\left(-\frac{\lambda_p L_p}{c^{\mathrm{P}} m_{p,t}}\right) + T_t^{\mathrm{A}}, \tag{4w}$$

$$\sum_{p \in S_n^{\mathrm{P,e}}} \left(m_{p,t} T_{p,t}^{\mathrm{out}}\right) = \sum_{p \in S_n^{\mathrm{P,e}}} (m_{p,t}) T_{n,t}^{\mathrm{mix}}, \tag{4x}$$

$$T_{p,t}^{\mathrm{in}} = T_{n,t}^{\mathrm{mix}} \ \ \forall p \in S_n^{\mathrm{P,s}}. \tag{4y}$$

(4u) and (4v) impose heat energy exchanges at heat source and load nodes, respectively. (4w) denotes the temperature drop along pipelines. (4x) states mixture temperatures at confluence nodes. (4y) ensures the same temperature for the mass outflows at a confluence node.

III. Proposed Solution Methodology

We begin in this section by presenting the model in vector/matrix forms. We then drive the reformulation of the DR model with the strengthened ambiguity set. Finally, we present the modified column-and-constraint generation algorithm.

A. Compact Formulation

For notational brevity, we express the DR model (4a)–(4y) in vectors and matrices as

$$\min_{\mathbf{x}} \ \mathbf{c}^T \mathbf{x} + \sup_{\mathrm{P} \in F} \mathrm{E}_{\mathrm{P}}\left[Q(\mathbf{x},\mathbf{z})\right], \tag{5a}$$

$$\text{s.t. } \mathbf{A}\mathbf{x} \le \mathbf{b}, \tag{5b}$$

where

$$Q(\mathbf{x},\mathbf{z}) = \min_{\mathbf{y}} \mathbf{d}^T\mathbf{y}, \tag{5c}$$

$$\text{s.t. } \mathbf{E}\mathbf{x}+\mathbf{G}\mathbf{y}+\mathbf{M}\mathbf{z} \le \mathbf{h}. \tag{5d}$$

(4a), (4b)–(4d), (4e), and (4f)–(4y) are represented in (5a), (5b), (5c), and (5d), respectively. The ambiguity set F (3a) and the support set Ω (3b) are also represented as

$$F = \left\{ \mathrm{P} \in P(\Omega) \;\middle|\; \begin{array}{l} \mathrm{E_P}(\mathbf{1}-\mathbf{z}) \le \mathbf{p} \\ d_W(\mathrm{P},\mathrm{P^E}) \le \theta \end{array} \right\}, \tag{5e}$$

$$\Omega = \left\{ \mathbf{z} \in \mathrm{R}^I \,|\mathbf{I}\mathbf{z} \le \mathbf{j} \right\}. \tag{5f}$$

B. Problem Reformulation

We first rewrite the Wasserstein metric (3c) as

$$\begin{aligned} d_W(\mathrm{P},\mathrm{P^E}) &= \inf_{\Pi} \left\{ \int_{\mathbf{z}\in\Omega}\int_{\mathbf{z}^\mathrm{E}\in\Omega} \left\|\mathbf{z}-\mathbf{z}^\mathrm{E}\right\| \Pi\left(d\mathbf{z}, d\mathbf{z}^\mathrm{E}\right) \right\} \\ &= \inf_{\mathrm{P}_s} \left\{ \sum_s \int_{\mathbf{z}\in\Omega} p_s \left\|\mathbf{z}-\mathbf{z}_s^\mathrm{E}\right\| \mathrm{P}_s(d\mathbf{z}) \right\}. \end{aligned} \tag{6a}$$

This reformulation applies the conditional distribution

$$\Pi\left(d\mathbf{z}, d\mathbf{z}^\mathrm{E}\right) = p_s \mathrm{P}_s(d\mathbf{z}), \tag{6b}$$

where $\mathrm{P}_s(\mathrm{d}\mathbf{z})$ is the conditional distribution of P when $\mathbf{z}^\mathrm{E} = \mathbf{z}_s^\mathrm{E}$. Then, we rewrite the second-stage supremum term in (5a) as

$$\begin{aligned} \sup_{\mathrm{P}\in F} \mathrm{E_P}\left[Q(\mathbf{x},\mathbf{z})\right] &= \max_{\mathrm{P}} \int_{\mathbf{z}\in\Omega} Q(\mathbf{x},\mathbf{z})\mathrm{P}(d\mathbf{z}) \\ &= \max_{\mathrm{P}_s} \sum_s \int_{\mathbf{z}\in\Omega} p_s Q(\mathbf{x},\mathbf{z})\mathrm{P}_s(d\mathbf{z}). \end{aligned} \tag{6c}$$

This reformulation employs the law of total probability

$$\mathrm{P}(d\mathbf{z}) = \sum_s p_s \mathrm{P}_s(d\mathbf{z}). \tag{6d}$$

The law of total probability (6d) is also employed to rewrite the moment constraint in (5e) as

$$\begin{aligned} \mathrm{E_P}(\mathbf{1}-\mathbf{z}) &= \int_{\mathbf{z}\in\Omega} (\mathbf{1}-\mathbf{z})\mathrm{P}(d\mathbf{z}) \\ &= \sum_s \int_{\mathbf{z}\in\Omega} p_s\,(\mathbf{1}-\mathbf{z})\mathrm{P}_s(d\mathbf{z}). \end{aligned} \tag{6e}$$

In this context, the second-stage supremum term with $\mathbf{z}$ subject to the ambiguity set F (5e) can be transformed into the semi-infinite formulation with dual variables α_s , $\boldsymbol{\beta}$, and γ as

$$\max_{\mathrm{P}_s} \sum_s \int_{\mathbf{z}\in\Omega} p_s Q(\mathbf{x},\mathbf{z})\mathrm{P}_s(d\mathbf{z}) \tag{6f}$$

$$\text{s.t. } \int_{\mathbf{z}\in\Omega} \mathrm{P}_s(d\mathbf{z}) = \mathbf{1} \quad : \alpha_s \tag{6g}$$

$$\sum_s \int_{\mathbf{z}\in\Omega} p_s\,(\mathbf{1}-\mathbf{z})\mathrm{P}_s(d\mathbf{z}) \le \mathbf{p} \quad : \boldsymbol{\beta} \tag{6h}$$

$$\sum_s \int_{\mathbf{z}\in\Omega} p_s \left\|\mathbf{z}-\mathbf{z}_s^\mathrm{E}\right\| \mathrm{P}_s(d\mathbf{z}) \le \theta \quad : \gamma \tag{6i}$$

The feasible region of the problem (6f)–(6i) has at least an interior point with $\mathrm{P}_s(d\mathbf{z}) = \delta(\mathbf{z}_s^\mathrm{E})$. Therefore, the Slater's condition holds, and the problem (6f)–(6i) can be transformed into the following equivalent minimization problem.

$$\min_{\alpha_s,\boldsymbol{\beta}\ge 0,\gamma\ge 0} \sum_s p_s\alpha_s + \mathbf{p}^T\boldsymbol{\beta} + \theta\gamma \tag{6j}$$

$$\text{s.t. } \alpha_s + \boldsymbol{\beta}^T(\mathbf{1}-\mathbf{z}) + \gamma\left\|\mathbf{z}-\mathbf{z}_s^\mathrm{E}\right\| \ge Q(\mathbf{x},\mathbf{z}) \;\; \forall \mathbf{z}\in\Omega \tag{6k}$$

We further reformulate (6k) as

$$\alpha_s + \mathbf{1}^T\boldsymbol{\beta} \ge \min_{\|\boldsymbol{\varepsilon}_s\|_*\le\gamma} \max_{\mathbf{z}\in\Omega} \left[Q(\mathbf{x},\mathbf{z}) + \boldsymbol{\beta}^T\mathbf{z} - \varepsilon_s^T\left(\mathbf{z}-\mathbf{z}_s^\mathrm{E}\right)\right], \tag{6l}$$

where $\boldsymbol{\varepsilon}_s$ denotes the introduced auxiliary variables and $\|\cdot\|_*$ represents the dual norm operator (detailed derivation is provided in the Appendix). Note that the dual norm of the l_1 norm adopted in this paper is the l_∞ norm. Finally, replacing the supremum term in (5a) with (6j) and (6l) yields the following equivalent formulation of the original DR model (5a)–(5d):

$$\min_{\mathbf{x},\alpha_s,\boldsymbol{\beta}\ge 0,\gamma\ge 0,\boldsymbol{\varepsilon}_s} \mathbf{c}^T\mathbf{x} + \sum_s p_s\alpha_s + (\mathbf{p}-\mathbf{1})^T\boldsymbol{\beta} + \theta\gamma, \tag{6m}$$

$$\text{s.t. } \mathbf{A}\mathbf{x} \le \mathbf{b}, \tag{6n}$$

$$\|\boldsymbol{\varepsilon}_s\|_* \le \gamma, \tag{6o}$$

$$\alpha_s \ge \max_{\mathbf{z}\in\Omega} \left[Q(\mathbf{x},\mathbf{z}) + \boldsymbol{\beta}^T\mathbf{z} - \varepsilon_s^T\left(\mathbf{z}-\mathbf{z}_s^\mathrm{E}\right)\right], \tag{6p}$$

where

$$Q(\mathbf{x},\mathbf{z}) = \min_{\mathbf{y}} \mathbf{d}^T\mathbf{y}, \tag{6q}$$

$$\text{s.t. } \mathbf{E}\mathbf{x}+\mathbf{G}\mathbf{y}+\mathbf{M}\mathbf{z} \le \mathbf{h}. \tag{6r}$$

C. Modified Column-and-Constraint Generation Algorithm

The recast DR model (6m)–(6r) is similar to a conventional two-stage robust model, and therefore can be solved by any methods demonstrated to be available for the latter, such as Benders decomposition and column-and-constraint generation algorithms. Here, we employ the column-and-constraint generation algorithm [35], which outperforms Benders decomposition in the convergence performance and computational efficiency. Furthermore, we modify the column-and-constraint generation algorithm to make it applicable to the recast DR model (6m)–(6r). The modified algorithm differs from the conventional one in two aspects: 1) each iteration includes N^S subproblems, and 2) solutions of the subproblems depend not only on the first-stage variables $\mathbf{x}$ but also on the dual variables $\boldsymbol{\beta}$ and auxiliary variables $\boldsymbol{\varepsilon}_s$.

The second-stage linear problem (6q) and (6r) is always feasible and bounded because this problem allows load shedding and aims at minimizing the total operation cost. In this regard, the strong duality holds, and the problem (6q) and (6r) can be equivalently converted into its dual formulation:

$$Q(\mathbf{x},\mathbf{z}) = \max_{\boldsymbol{\pi}\le 0} (\mathbf{h}-\mathbf{E}\mathbf{x}-\mathbf{M}\mathbf{z})^T\boldsymbol{\pi}, \tag{7a}$$

$$\text{s.t. } \mathbf{G}^T\boldsymbol{\pi} = \mathbf{d}, \tag{7b}$$

where $\boldsymbol{\pi}$ is the dual variables of (6r). The bilinear terms $\mathbf{z}^T\mathbf{M}^T\boldsymbol{\pi}$ in (7a) can be linearized by McCormick inequalities [21]. Note that the performance of McCormick inequalities is exact for the bilinear terms $\mathbf{z}^T\mathbf{M}^T\boldsymbol{\pi}$ with binary variables $\mathbf{z}$.

The procedure for the modified column-and-constraint generation algorithm is detailed as follows.

Step 0: Specify an initial branch outage set $Z = \{\mathbf{z}_{0,s}\}$ and a convergence tolerance ϵ. Set the lower bound LB to $-\infty$, the upper bound UB to $+\infty$, and the iteration counter $c = 1$.

Step 1: Solve the following master problem.

$$\min_{\mathbf{x},\alpha_s,\boldsymbol{\beta}\geq 0,\gamma\geq 0,\boldsymbol{\varepsilon}_s,\mathbf{y}_{c,s}} \mathbf{c}^T\mathbf{x} + \sum_s p_s\alpha_s + (\mathbf{p}-\mathbf{1})^T\boldsymbol{\beta} + \theta\gamma \tag{7c}$$

$$\text{s.t. } \mathbf{A}\mathbf{x} \leq \mathbf{b} \tag{7d}$$

$$\|\boldsymbol{\varepsilon}_s\|_* \leq \gamma \tag{7e}$$

$$\alpha_s \geq \mathbf{d}^T\mathbf{y}_{l,s} + \boldsymbol{\beta}^T\mathbf{z}_{l,s} - \varepsilon_s^T\left(\mathbf{z}_{l,s} - \mathbf{z}_s^{\mathrm{E}}\right) \quad \forall l < c \tag{7f}$$

$$\mathbf{E}\mathbf{x} + \mathbf{G}\mathbf{y}_{l,s} + \mathbf{M}\mathbf{z}_{l,s} \leq \mathbf{h} \quad \forall l < c \tag{7g}$$

Let $(\mathbf{x}_c,\ \alpha_{c,s},\ \boldsymbol{\beta}_c,\ \gamma_c,\ \boldsymbol{\varepsilon}_{c,s})$ and V_c^{MP} be the solution and objective value of the master problem, and update $LB = V_c^{\mathrm{MP}}$.

Step 2: Solve N^{S} subproblems based on the optimal solution of the master problem obtained in Step 1. Subproblem s is given as follows.

$$\max_{\mathbf{z},\boldsymbol{\pi}\leq 0} (\mathbf{h} - \mathbf{E}\mathbf{x}_c - \mathbf{M}\mathbf{z})^T\boldsymbol{\pi} + \boldsymbol{\beta}_c^T\mathbf{z} - \varepsilon_{c,s}^T\left(\mathbf{z} - \mathbf{z}_s^{\mathrm{E}}\right) \tag{7h}$$

$$\text{s.t. } \mathbf{I}\mathbf{z} \leq \mathbf{j} \tag{7i}$$

$$\mathbf{G}^T\boldsymbol{\pi} = \mathbf{d} \tag{7j}$$

Let $(\mathbf{z}_{c,s}, \boldsymbol{\pi}_{c,s})$ and $V_{c,s}^{\mathrm{SP}}$ be the solution and objective value of subproblem s, and update $UB = \min\{UB, \mathbf{c}^T\mathbf{x}_c + \sum_s p_s V_{c,s}^{\mathrm{SP}} + (\mathbf{p}-\mathbf{1})^T\boldsymbol{\beta}_c + \theta\gamma_c\}$.

Step 3: If $(UB - LB)/LB < \epsilon$, present the results and terminate the procedure; otherwise, update $Z = Z \cup \{\mathbf{z}_{c,s}\}$ and $c = c + 1$, and return to Step 1.

Note that the dual variables associated with (7f) are $\mathrm{P}_s(\mathrm{d}\boldsymbol{\varepsilon})$. Those dual variables reveal the worst-case distribution of branch outages. That is, we can obtain the worst-case distribution of uncertain parameters straightforwardly by the modified column-and-constraint generation algorithm, which cannot be achieved when employing linear decision rules. Besides, since the second-stage problem is linear and always feasible, the column-and-constraint generation algorithm could be terminated in a finite number of iterations [35].

IV. Case Study

In this section, we first study a 4-bus and 5-node integrated energy distribution system as an illustrative example to validate the effectiveness of the proposed DR approach. Then, a 33-bus and 32-node integrated energy distribution system is tested to show the performance of the strengthened ambiguity set and the computational efficiency of the modified column-and-constraint generation algorithm. Finally, a 123-bus and 32-node integrated energy distribution system is conducted to examine the scalability of the proposed approach. All three coupled systems are modified from [36], with detailed system data available in [37]. For simplicity, case studies are implemented under normal load conditions. However, the validity of the proposed approach will not be affected by the amount of load.

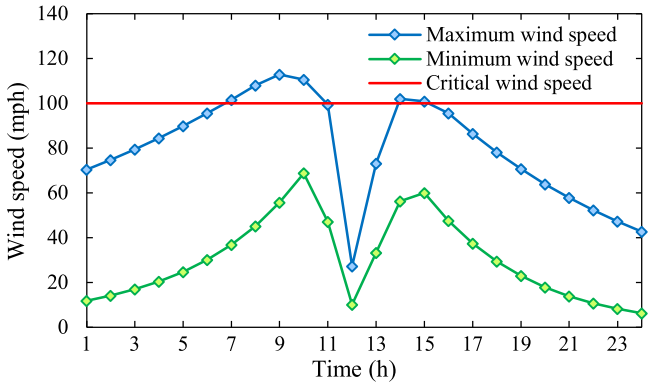

Fig. 2. Comparison of distribution system wind speeds with critical wind speed.

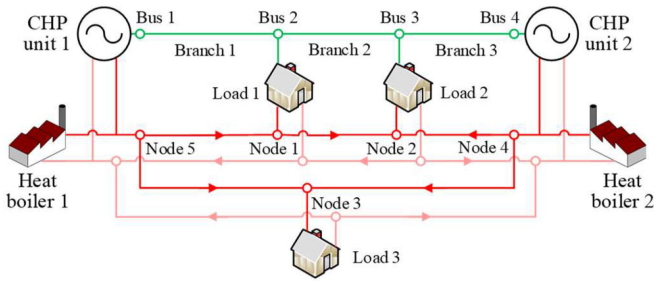

Fig. 3. Topology of 4-bus and 5-node integrated energy distribution system.

The sample generation method of time-varying hurricane parameters and hurricane eye locations are detailed in [24]. In addition, the fragility curve of branch poles is obtained from [38]. Here, we assume all poles share the same fragility curve. Fig. 2 shows a comparison of maximum and minimum wind speeds at the distribution system on a hurricane day and the critical wind speed leading to pole outages based on the fragility curve. The hurricane would damage branches when the wind speed at the distribution system exceeds the critical wind speed. This means that branches may be damaged only in period 7 or later during this hurricane.

All experiments are implemented on a personal computer with a 3.2 GHz Intel Core i7 CPU and 8 GB memory. All optimization models are performed using the CPLEX solver on the GAMS platform. The confidence level η of the Wasserstein radius is set to 95%. The convergence tolerance ϵ of the column-and-constraint generation algorithm is set to 10^{-3}.

A. 4-Bus and 5-Node System

Fig. 3 depicts the topology of the 4-bus and 5-node integrated electricity and heat energy distribution system, which includes two CHP units and two heat boilers.

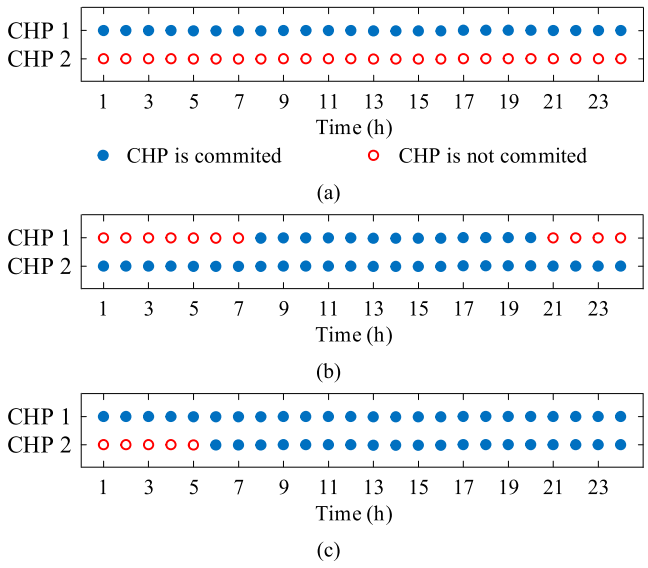

Fig. 4. CHP unit commitment decisions obtained by (a) deterministic approach, (b) conventional robust approach, and (c) proposed DR approach.

First, we compare the results of the proposed DR approach with those of the deterministic and the conventional robust approaches. In the deterministic approach, day-ahead unit commitment decisions of CHP units are decided without considering those contingencies caused by the upcoming hurricane. That is, no preventive measures are implemented in the deterministic approach. In the DR approach, the ambiguity set is constructed using 50 branch outage samples, considering the sparsity of historical hurricane data. We observe that the maximum branch outage number in these samples is 1. Thus, $N-1$ contingencies are considered here.

CHP unit commitment decisions obtained by the deterministic, the conventional robust, and the proposed DR approaches are presented in Fig. 4(a), (b), and (c), respectively. Here, only the CHP unit 1 is employed by the deterministic approach because it is the cheaper unit and is therefore used exclusively to reduce the operation cost. The conventional robust approach always commits the CHP unit 2 and partially leaves the CHP unit 1 uncommitted, which is prepared for the worst-case scenario where branch 1 is damaged. In the DR approach, the CHP unit 1 is always committed and the CHP unit 2 is generally committed to protecting the system against all possible scenarios with the distribution in the ambiguity set.

The adaptability of unit commitment decisions obtained by the three optimization approaches to the impending hurricane is tested under three extreme scenarios, where branches 1, 2, and 3 are damaged separately. The damage period is 7, which is the most serious period in this hurricane (see Fig. 2). The actual costs for these branch outage scenarios are calculated by the second-stage model (4e)–(4y) with fixed unit commitment decisions and branch outage scenarios.

The solution results are listed in Table I. The deterministic approach suffers very large economic losses corresponding to load shedding when branch 1 or 2 is damaged. This is because the deterministic approach neglects the influence of the hurricane and applies no preventive measures. In this situation, the system is highly vulnerable to the hurricane. The conventional robust approach performs better than the deterministic approach in terms of load shedding costs with damaged branches 1 and 2. However, this approach focuses only on the worst-case scenario (i.e., damaged branch 1), which may lead to poor performances in practice if other scenarios occur, such as damaged branch 3 in the test. In comparison, the DR approach accommodates all possible occurrences of branch outages with the distribution in the ambiguity set and thereby effectively mitigates serious load shedding events in each scenario, although with relatively high CHP unit costs. In particular, the load shedding costs of the DR approach are 0 under the conditions of branches 2 and 3 outages.

TABLE I
ACTUAL COSTS OF THREE OPTIMIZATION APPROACHES UNDER DIFFERENT BRANCH OUTAGE SCENARIOS

Approach	Outage branch	Cost ($)			
		CHP unit	Heat boiler	Load shedding	Total
Deterministic	1	73.52	17.88	7035.58	7126.98
	2	80.19	15.88	3517.79	3613.85
	3	96.79	21.35	0	118.14
Conventional robust	1	101.15	26.11	3159.52	3286.78
	2	111.72	14.59	954.95	1081.26
	3	110.75	18.42	1983.46	2112.64
Proposed DR	1	119.76	17.28	2985.58	3122.61
	2	130.56	5.85	0	136.41
	3	135.07	10.05	0	145.12

TABLE II
AVERAGE COSTS OF THREE OPTIMIZATION APPROACHES

Approach	Cost ($)			
	CHP unit	Heat boiler	Load shedding	Total
Deterministic	84.82	18.35	3209.39	3312.57
Conventional robust	108.24	19.76	1873.84	2001.84
Proposed DR	128.47	10.47	926.46	1065.40

We further implement out-of-sample simulations. Here, 100 out-of-sample scenarios with damaged branches are employed. The results are listed in Table II. The average total cost of the DR approach is 67.84% and 46.78% less than those of the deterministic and conventional robust approaches, respectively.

In general, the proposed DR approach is effective in reducing load shedding and enhancing the resilience of the integrated electricity and heat energy distribution system against the upcoming hurricane.

B. 33-Bus and 32-Node System

The system composed of the IEEE 33-bus PDN and the Barry Island 32-node DHN is tested here, with the topology depicted in Fig. 5. $N-3$ contingencies are considered for this system based on the generated branch outage samples.

1) Performance of Strengthened Ambiguity Set: Three different DR approaches that employ either the moment-based,

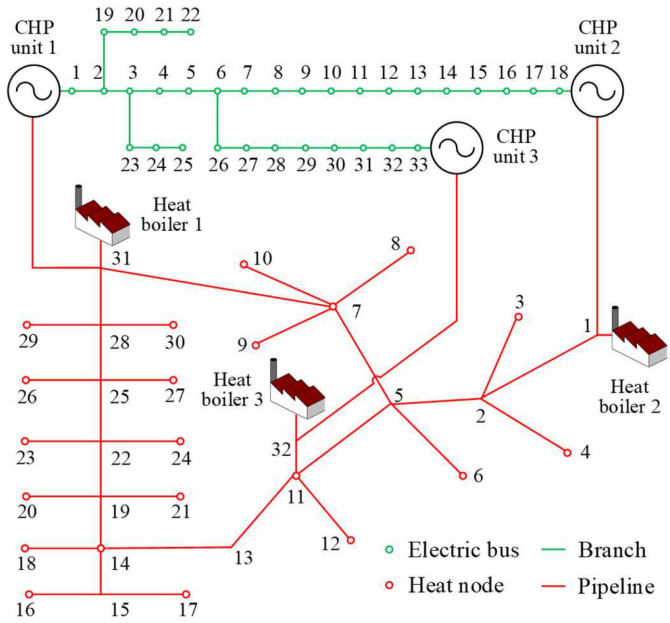

Fig. 5. Topology of 33-bus and 32-node integrated energy distribution system.

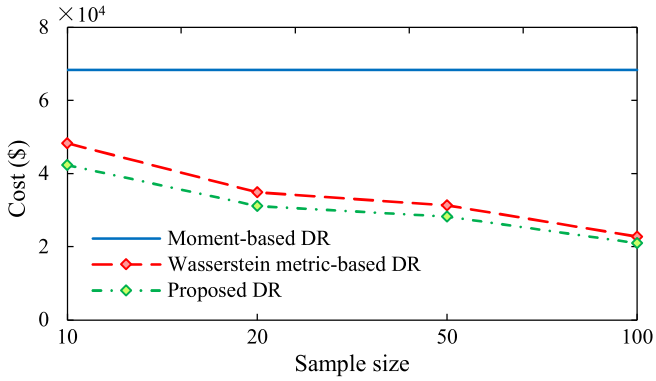

Fig. 6. Objective values of three DR approaches with different sample sizes.

the Wasserstein metric-based, or the proposed strengthened ambiguity sets are investigated, and their objective values are presented in Fig. 6. The moment-based DR approach is somewhat conservative and cannot reduce the objective value with an increasing number of the samples because the moment information alone is insufficient to characterize the true distribution fully. By comparison, the Wasserstein metric-based and the proposed DR approach are less conservative, and their objective values can be reduced gradually with the increasing sample size. This is because these two approaches incorporate a variety of historical data to enhance the characterization of the true probability distribution. Accordingly, the true distribution is revealed with increasing accuracy as the number of available data increases, which reduces the size of the ambiguity set by excluding improbable distributions. Moreover, the proposed DR approach is less conservative than the Wasserstein metric-based DR approach for any sample size because it also includes moment information, which expands the level of available probability distribution data. These results verify the ability of the proposed DR approach for employing a wind range of data to provide a more comprehensive characterization of the true probability distribution, and thereby obtains more trustworthy and less conservative solutions.

TABLE III
COMPUTATIONAL EFFICIENCY OF THREE DR MODELS WITH DIFFERENT SAMPLE SIZES

Model	Efficiency	Sample size			
		10	20	50	100
Moment	Iteration	77			
	Time (min)	32.87			
Wasserstein	Iteration	5	5	5	5
	Time (min)	0.73	0.93	2.02	4.17
Proposed	Iteration	38	30	22	17
	Time (min)	19.78	21.65	25.88	36.83

TABLE IV
OBJECTIVE VALUES AND COMPUTATIONAL EFFICIENCY OF THREE DR MODELS

Model	Objective (k$)	Iteration	Time (min)
Moment	401.40	70	84.42
Wasserstein	164.82	5	24.27
Proposed	144.63	18	118.95

2) Computational Efficiency Analysis: Table III reports the computational efficiency of the moment-based, the Wasserstein metric-based, and the proposed DR models solved by column-and-constraint generation algorithms. The proposed DR model takes less time than the moment-based one when the sample size is small, owing to the requirement of fewer interactions. Nevertheless, the computation time of the proposed DR model increases as the sample size increases and exceeds that of the moment-based DR model when the sample size is large (e.g., the sample size $N^{\mathrm{S}} = 100$). Besides, the proposed DR model is much more difficult to solve than the Wasserstein metric-based DR model, because more interactions are necessary.

The computation time of the proposed DR model increases slowly with the increasing sample size. This is because the size of the ambiguity set decreases as more historical data become available, such that fewer scenarios must be searched and fewer numbers of iterations are required. The fact that the incorporation of more historical data does not increase the computation time remarkably verifies the scalability of the proposed solution algorithm to the model.

C. 123-Bus and 32-Node System

We further conduct case studies on the system composed of the IEEE 123-bus PDN and the Barry Island 32-node DHN. Three CHP units are connected to buses 1, 114, and 96 in the PDN and nodes 31, 1, and 32 in the DHN. Three heat boilers are located at the same nodes as the CHP units.

Table IV lists the objective values and the computational efficiency of the moment-based, the Wasserstein metric-based, and the proposed DR models, with the simple size $N^{\mathrm{S}} = 50$ as an example. The proposed DR model obtains a lower objective value than those of the moment-based and the Wasserstein metric-based DR models, which demonstrates the effectiveness

of the proposed DR approach in reducing the conservatism for large-scale systems. Besides, the computation time of the proposed DR model is shorter than 2h, which is generally compatible with the day-ahead scheduling requirements. Unlike the computation time, the number of iterations is insensitive to the system scale, represented by similar numbers of interactions on this system and the 33-bus and 32-node system. This implies that the modified column-and-constraint generation algorithm offers a scalable solvability to the proposed model.

V. Conclusion

This paper proposes a DR model for the resilient operation of integrated electricity and heat energy distribution systems in extreme weather events. The proposed DR model adopts a strengthened ambiguity set that incorporates both moment and Wasserstein metric information. The proposed model is recast into a framework similar to a conventional two-stage robust model and is solved by a modified column-and-constraint generation algorithm. Numerical results validate the effectiveness of the DR approach for enhancing the resilience of the integrated electricity and heat energy distribution systems. The results also demonstrate that the incorporation of both moment and Wasserstein metric information into the strengthened ambiguity set reduces the conservatism of solutions. Moreover, the modified column-and-constraint generation algorithm is demonstrated to provide scalable solutions. The future work includes: 1) considering the restoration progress of integrated energy distribution systems after hurricanes, 2) incorporating distribution network reconfiguration with remotely controlled switches, and 3) solving subproblems simultaneously in each iteration by parallel computing techniques.

Appendix

This section provides the step-by-step derivation from (6k) to (6l). First, we rewrite (6k) as the following worst-case expression:

$$\alpha_s + \mathbf{1}^T\boldsymbol{\beta} \geq \max_{\mathbf{z}\in\Omega} \left[Q(\mathbf{x},\mathbf{z}) + \boldsymbol{\beta}^T\mathbf{z} - \gamma \left\|\mathbf{z}-\mathbf{z}_s^{\mathrm{E}}\right\|\right]. \tag{8a}$$

The right-hand side of (8a) can be reformulated as

$$\max_{\mathbf{z}\in\Omega}\left[Q(\mathbf{x},\mathbf{z}) + \boldsymbol{\beta}^T\mathbf{z} - \max_{\|\boldsymbol{\varepsilon}_s\|_*\leq\gamma} \varepsilon_s^T\left(\mathbf{z}-\mathbf{z}_s^{\mathrm{E}}\right)\right], \tag{8b}$$

according to the definition of the dual norm

$$\left\|\mathbf{z}-\mathbf{z}_s^{\mathrm{E}}\right\| = \max_{\|\boldsymbol{\varepsilon}_s\|_*\leq 1} \varepsilon_s^T\left(\mathbf{z}-\mathbf{z}_s^{\mathrm{E}}\right). \tag{8c}$$

Then, interchanging the maximization over ε_s with the minus sign, and thus converting the maximization to a minimization, we reformulate (8b) as

$$\max_{\mathbf{z}\in\Omega}\min_{\|\boldsymbol{\varepsilon}_s\|_*\leq\gamma}\left[Q(\mathbf{x},\mathbf{z}) + \boldsymbol{\beta}^T\mathbf{z} - \varepsilon_s^T\left(\mathbf{z}-\mathbf{z}_s^{\mathrm{E}}\right)\right]. \tag{8d}$$

Finally, we rewrite (8d) based on the minimax theorem as

$$\min_{\|\boldsymbol{\varepsilon}_s\|_*\leq\gamma}\max_{\mathbf{z}\in\Omega}\left[Q(\mathbf{x},\mathbf{z}) + \boldsymbol{\beta}^T\mathbf{z} - \varepsilon_s^T\left(\mathbf{z}-\mathbf{z}_s^{\mathrm{E}}\right)\right]. \tag{8e}$$

References

[1] "Economic benefits of increasing electric grid resilience to weather outages," Executive Office of the President, WA, DC, USA: Tech. Rep., Aug. 2013.

[2] "Billion-Dollar weather and climate disasters: Overview," Jun. 2020. [Online]. Available: https://www.ncdc.noaa.gov/billions/

[3] R. Li, W. Wei, S. Mei, Q. Hu, and Q. Wu, "Participation of an energy hub in electricity and heat distribution markets: An MPEC approach," *IEEE Trans. Smart Grid,* vol. 10, no. 4, pp. 3641–3653, Jul. 2019.

[4] W. Yuan, J. Wang, F. Qiu, C. Chen, C. Kang, and B. Zeng, "Robust optimization-based resilient distribution network planning against natural disasters," *IEEE Trans. Smart Grid,* vol. 7, no. 6, pp. 2817–2826, Nov. 2016.

[5] S. Ma, B. Chen, and Z. Wang, "Resilience enhancement strategy for distribution systems under extreme weather events," *IEEE Trans. Smart Grid,* vol. 9, no. 2, pp. 1442–1451, Mar. 2018.

[6] M. H. Amirioun, F. Aminifar, and M. Shahidehpour, "Resilience-promoting proactive scheduling against hurricanes in multiple energy carrier microgrids," *IEEE Trans. Power Syst.,* vol. 34, no. 3, pp. 2160–2168, May 2019.

[7] C. Shao, M. Shahidehpour, X. Wang, X. Wang, and B. Wang, "Integrated planning of electricity and natural gas transportation systems for enhancing the power grid resilience," *IEEE Trans. Power Syst.,* vol. 32, no. 6, pp. 4418–4429, Nov. 2017.

[8] M. Yan, Y. He, M. Shahidehpour, X. Ai, Z. Li, and J. Wen, "Coordinated regional-district operation of integrated energy systems for resilience enhancement in natural disasters," *IEEE Trans. Smart Grid,* vol. 10, no. 5, pp. 4881–4892, Sep. 2019.

[9] Y. Li, Z. Li, F. Wen, and M. Shahidehpour, "Minimax-regret robust co-optimization for enhancing the resilience of integrated power distribution and natural gas systems," *IEEE Trans. Sustain. Energy,* vol. 11, no. 1, pp. 61–71, Jan. 2020.

[10] X. Zhang, M. Shahidehpour, A. Alabdulwahab, and A. Abusorrah, "Hourly electricity demand response in the stochastic day-ahead scheduling of coordinated electricity and natural gas networks," *IEEE Trans. Power Syst.,* vol. 31, no. 1, pp. 592–601, Jan. 2016.

[11] S. Chen, Z. Wei, G. Sun, K. W. Cheung, D. Wang, and H. Zang, "Adaptive robust day-ahead dispatch for urban energy systems," *IEEE Trans. Ind. Electron.,* vol. 66, no. 2, pp. 1379–1390, Feb. 2019.

[12] Y. Zhou, Z. Wei, G. Sun, K. W. Cheung, H. Zang, and S. Chen, "A robust optimization approach for integrated community energy system in energy and ancillary service markets," *Energy,* vol. 148, pp. 1–15, Apr. 2018.

[13] E. Delage and Y. Ye, "Distributionally robust optimization under moment uncertainty with application to data-driven problems," *Oper. Res.,* vol. 58, no. 3, pp. 595–612, Jan. 2010.

[14] J. Goh and M. Sim, "Distributionally robust optimization and its tractable approximations," *Oper. Res.,* vol. 58, no. 4, pp. 902–917, Apr. 2010.

[15] P. Xiong, P. Jirutitijaroen, and C. Singh, "A distributionally robust optimization model for unit commitment considering uncertain wind power generation," *IEEE Trans. Power Syst.,* vol. 32, no. 1, pp. 39–49, Jan. 2017.

[16] W. Wei, F. Liu, and S. Mei, "Distributionally robust co-optimization of energy and reserve dispatch," *IEEE Trans. Sustain. Energy,* vol. 7, no. 1, pp. 289–300, Jan. 2016.

[17] C. Duan, W. Fang, L. Jiang, L. Yao, and J. Liu, "Distributionally robust chance-constrained approximate AC-OPF with Wasserstein metric," *IEEE Trans. Power Syst.,* vol. 33, no. 5, pp. 4924–4936, Sep. 2018.

[18] Y. Zhou, M. Shahidehpour, Z. Wei, Z. Li, G. Sun, and S. Chen, "Distributionally robust unit commitment in coordinated electricity and district heating networks," *IEEE Trans. Power Syst.,* vol. 35, no. 3, pp. 2155–2166, May 2020.

[19] C. He, X. Zhang, T. Liu, and L. Wu, "Distributionally robust scheduling of integrated gas-electricity systems with demand response," *IEEE Trans. Power Syst.,* vol. 34, no. 5, pp. 3791–3803, Sep. 2019.

[20] C. Wang, R. Gao, W. Wei, M. Shafie-khah, T. Bi, and J. P. S. Catalão, "Risk-based distributionally robust optimal gas-power flow with Wasserstein distance," *IEEE Trans. Power Syst.,* vol. 34, no. 3, pp. 2190–2204, May 2019.

[21] C. Zhao and R. Jiang, "Distributionally robust contingency-constrained unit commitment," *IEEE Trans. Power Syst.,* vol. 33, no. 1, pp. 94–102, Jan. 2018.

[22] S. Babaei, R. Jiang, and C. Zhao, "Distributionally robust distribution network configuration under random contingency," *IEEE Trans. Power Syst.,* vol. 35, no. 5, pp. 3332–3341, Sept. 2020.

[23] G. Li *et al.*, "Risk analysis for distribution systems in the northeast U.S. under wind storms," *IEEE Trans. Power Syst.,* vol. 29, no. 2, pp. 889–898, Mar. 2014.
[24] P. Javanbakht and S. Mohagheghi, "A risk-averse security-constrained optimal power flow for a power grid subject to hurricanes," *J. Elect. Power Syst. Res.,* vol. 116, pp. 408–418, Nov. 2014.
[25] X. Chen *et al.*, "Increasing the flexibility of combined heat and power for wind power integration in China: Modeling and implications," *IEEE Trans. Power Syst.*, vol. 30, no. 4, pp. 1848–1857, Jul. 2015.
[26] H. Yeh, D. F. Gayme, and S. H. Low, "Adaptive VAR control for distribution circuits with photovoltaic generators," *IEEE Trans. Power Syst.*, vol. 27, no. 3, pp. 1656–1663, Aug. 2012.
[27] G. Sun, S. Chen, Z. Wei, K. W. Cheung, and H. Zang, "Corrective security-constrained optimal power and gas flow with binding contingency identification," *IEEE Trans. Sustain. Energy,* vol. 11, no. 2, pp. 1033–1042, Apr. 2020.
[28] Y. Cao, W. Wei, J. Wang, S. Mei, M. Shafie-khah, and J. P. S. Catalão, "Capacity planning of energy hub in multi-carrier energy networks: A data-driven robust stochastic programming approach," *IEEE Trans. Sustain. Energy,* vol. 11, no. 1, pp. 3–14, Jan. 2020.
[29] Z. Li, W. Wu, J. Wang, B. Zhang, and T. Zheng, "Transmission-constrained unit commitment considering combined electricity and district heating networks," *IEEE Trans. Sustain. Energy,* vol. 7, no. 2, pp. 480–492, Apr. 2016.
[30] Y. Zhou, M. Shahidehpour, Z. Wei, Z. Li, G. Sun, and S. Chen, "Distributionally robust co-optimization of energy and reserve for combined distribution networks of power and district heating," *IEEE Trans. Power Syst.,* vol. 35, no. 3, pp. 2388–2398, May 2020.
[31] S. Lu, W. Gu, K. Meng, S. Yao, B. Liu, and Z. Y. Dong, "Thermal inertial aggregation model for integrated energy systems," *IEEE Trans. Power Syst.,* vol. 35, no. 3, pp. 2374–2387, May 2020.
[32] S. Lu, W. Gu, C. Zhang, K. Meng, and Z. Y. Dong, "Hydraulic-thermal cooperative optimization of integrated energy systems: A convex optimization approach," *IEEE Trans. Smart Grid,* vol. 11, no. 6, pp. 4818–4832, Nov. 2020.
[33] C. Shao, Y. Ding, P. Siano, and Z. Lin, "A framework for incorporating demand response of smart buildings into the integrated heat and electricity energy system," *IEEE Trans. Ind. Electron.,* vol. 66, no. 2, pp. 1465–1475, Feb. 2019.
[34] C. Shao, Y. Ding, J. Wang, and Y. Song, "Modeling and integration of flexible demand in heat and electricity integrated energy system," *IEEE Trans. Sustain. Energy,* vol. 9, no. 1, pp. 361–370, Jan. 2018.
[35] B. Zeng and L. Zhao, "Solving two-stage robust optimization problems using a column-and-constraint generation method," *Oper. Res. Lett.,* vol. 41, no. 5, pp. 457–461, Sep. 2013.
[36] X. Liu, "Combined analysis of electricity and heat networks," Ph.D. dissertation, Dept. Inst. Energy, Cardiff Univ., Cardiff, Wales, U.K., 2013.
[37] "Integrated energy distribution systems," Jun. 2020, doi: 10.6084/m9.figshare.12523439.v2.
[38] A. Shafieezadeh, U. P. Onyewuchi, M. M. Begovic, and R. DesRoches, "Age-dependent fragility models of utility wood poles in power distribution networks against extreme wind hazards," *IEEE Trans. Power Del.,* vol. 29, no. 1, pp. 131–139, Feb. 2014.

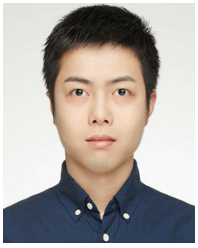

Yizhou Zhou (Member, IEEE) received the B.S. and Ph.D. degrees from the College of Energy and Electrical Engineering, Hohai University, Nanjing, China, in 2015 and 2020, respectively. From October 2018 to October 2019, he was a Visiting Scholar with the Illinois Institute of Technology, Chicago, IL, USA.

He is currently an Assistant Professor with the College of Energy and Electrical Engineering, Hohai University. His research interests include integrated energy systems, power system operation and planning, and electricity markets.

Zhinong Wei (Member, IEEE) received the B.S. degree from the Hefei University of Technology, Hefei, China, in 1984, the M.S. degree from Southeast University, Nanjing, China, in 1987, and the Ph.D. degree from Hohai University, Nanjing, China, in 2004.

He is currently a Professor of electrical engineering with the College of Energy and Electrical Engineering, Hohai University. His research interests include integrated energy systems, state estimation, and smart distribution systems.

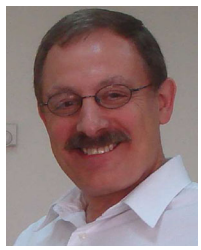

Mohammad Shahidehpour (Life Fellow, IEEE) received the Honorary Doctorate degree from the Polytechnic University of Bucharest, Bucharest, Romania. He is a University Distinguished Professor, and the Bodine Chair Professor and the Director of the Robert W. Galvin Center for Electricity Innovation, Illinois Institute of Technology, Chicago, IL, USA. He is a Member of the US National Academy of Engineering, a Fellow of the American Association for the Advancement of Science, and a Fellow of the National Academy of Inventors. He is listed as a highly cited researcher on the Web of Science (ranked in the top 1% by citations demonstrating significant influence among his peers).

Sheng Chen (Member, IEEE) received the B.S. and Ph.D. degrees from the College of Energy and Electrical Engineering, Hohai University, Nanjing, China, in 2014 and 2019, respectively. From January 2018 to January 2019, he was a Visiting Scholar with the Ohio State University, Columbus, OH, USA.

He is currently an Associate Professor with the College of Energy and Electrical Engineering, Hohai University. His current research interests include integrated energy systems, operations research, and electricity markets.